

# NUMERICAL 3D MODELLING OF ANCHORAGE, CORROSION AND SPALLING

Kamyab Zandi<sup>1,2</sup>, Karin Lundgren<sup>1</sup>

<sup>1</sup> Chalmers University of Technology, Department of Civil and Environmental Engineering, Concrete Structures, 412 96 Gothenburg, Sweden

<sup>2</sup> CBI Swedish Cement and Concrete Research Institute, Material Group, 501 15 Borås, Sweden

## Abstract

The aim of this study is to enhance our understanding of anchorage capacity in reinforced concrete structures with corrosion-induced cover spalling. Our objectives were to study the influence of corrosion-induced cover spalling on bond strength. Thus, earlier developed bond and corrosion models suited for detailed 3D finite element (FE) analysis were first combined with a new computation scheme to simulate corrosion-induced cover spalling. The 3D FE analyses were validated through experiments. The application of 3D FE analysis showed that the corrosion of stirrups advances the emergence of cracking and spalling, while bond strength is only slightly influenced by the corrosion of stirrups after cover spalling if early yielding of stirrups had not taken place. Moreover, it was shown that stresses in the stirrups due to corrosion in adjacent bars rapidly diminished within a short distance from the main bar, and that the corrosion of stirrups influenced the shear capacity more prominent than the induced stresses in stirrups due to the corrosion of main bars.

**Keywords:** Anchorage, Assessment, Corrosion, Bond-slip, Concrete, Reinforcement

## 1 Introduction

Infrastructures represent a large capital investment in all developed countries. To establish sustainable development, it is of great importance that infrastructures generate a return and that the investments result in safe structures with predictable performance. Despite significant advances in construction design and practice, corrosion in reinforced concrete (RC) structures is still a leading cause of deterioration worldwide (Sustainable Bridges, 2008). This situation has led to a growing demand for better assessment of existing concrete structures and has revealed a need for an improved understanding of the structural effects of corrosion.

The service life of reinforced concrete structures, according to the classical model of Tuutti (1982), is divided into two phases: initiation and propagation. The initiation phase is defined as the period leading to depassivation of steel governed by the critical chloride concentration at the depth of the reinforcement (Silva, 2013). Concerns about the structural integrity of reinforced concrete arise during the propagation period when corrosion leads to a reduction in the sectional area of reinforcing bars (Almusallam, 2001; Cairns et al., 2005), and a change in the ductility of steel bars (Du, 2001; Du et al., 2005). Furthermore, the volume expansion of corrosion products that generates splitting stresses in the concrete eventually cracks the surrounding concrete cover (Andrade et al., 1993; Rasheeduzzafar et al., 1992; Molina et al., 1993) and adversely affects the bond between the reinforcement and concrete (Al-Sulaimani et al., 1990; Cabrera & Ghoddoussi, 1992; Clark & Saifullah, 1993; fib, 2000; Lundgren, 2007; Sæther, 2009). For larger corrosion penetrations, the splitting stresses may lead to cover spalling (Coronelli et al., 2011) which alters the resisting mechanism in the cross-section (Cairns & Zhao, 1993; Regan & Kennedy Reid, 2009); stirrups then become the primary source of confinement (Zandi Hanjari, 2010). Therefore, the anchorage capacity of RC structures is influenced by cover cracking (Lundgren, 2007), cover spalling (Regan & Kennedy Reid, 2009), as well as by the

corrosion of stirrups (Higgins & Farrow III, 2006; Regan & Kennedy Reid, 2004). The structural behaviour of RC structures with corrosion-induced cracking have been examined in several earlier studies (Coronelli & Gambarova, 2004; Rodriguez et al., 1995; Almusallam et al., 1996; Zandi Hanjari et al., 2011b). However, the structural consequence of corrosion-induced cover spalling and corrosion of stirrups is not yet fully understood; these phenomena make up the primary focal points of the present study.

Cover spalling results in a decrease in the concrete cross-section and a loss of confinement. A reduction in the concrete cross-section leads to a decrease in the internal lever arm on the compressive side, which in turn decreases the bending moment (Rodriguez et al., 1997; Zandi Hanjari et al., 2011b). The loss of cover to, and full exposure of, tension reinforcement may change the structural behaviour from flexural to tied arch with secondary effects (Cairns & Zhao, 1993). Tests carried out on highly corroded beams with over 20% loss of bar weight have shown that relatively high residual load-carrying capacity was reached when corroded beams failed in bending (Azad et al., 2007; Zhang, 2008). Cover spalling may also reduce member resistance to shear cracking (Regan & Kennedy Reid, 2010). Nevertheless, it is the impact of cover spalling on bond capacity and anchorage behaviour which, in most cases, is of the highest concern. Regan and Kennedy Reid (2009) studied this by testing beams, cast without concrete covers, in which bars were either ‘flush’ with the concrete surface or exposed to ‘mid-barrel’. A reduction of the bond strength up to 90% was observed for the bars exposed to ‘mid-barrel’; however, the volume expansion of rust and the effect of corroded stirrups had not been taken into account. After all, the values indicative of the residual bond strength of corroded reinforcement given in Model Code 2010 (fib, 2013) cover only up to 5% corrosion weight loss, while the bond capacity for higher corrosion leading to cover spalling is still an open question. The present study represents an effort to address these concerns.

The aim of this study is to enhance our understanding of anchorage capacity in reinforced concrete structures with corrosion-induced cover spalling. The objectives of this paper was to study the effect of high corrosion attacks leading to cover spalling through the application of detailed numerical analysis. Thus, earlier developed bond and corrosion models suited for detailed 3D finite element (FE) analysis were first combined with a new computation scheme to simulate corrosion-induced cover spalling. The 3D FE analysis was both validated through two series of experiments and an empirical model available in the literature for the anchorage capacity of corroded RC structures with cover spalling. The 3D FE analysis was then used to further investigate the influence of stirrup corrosion, the corrosion distribution around a bar, and the induced stresses in stirrups caused by the corrosion of main bars.

## 2 Empirical model for anchorage after spalling

Most empirical models for the anchorage of corroded bar are primarily concerned with relatively low corrosion attacks. To the author’s knowledge, the only empirical model for the anchorage of bars with corrosion-induced cover spalling was proposed by Regan and Kennedy Reid (2009). Their model was based on pull-out, beam, slab and splice tests carried out on specimens cast without cover to the main bars, which were either ‘flush’ with the concrete surface or exposed to ‘mid-barrel’. Regardless of the length of the bar embedded in concrete, the nominal bond stress, defined as the change of bar force per unit length divided by  $\pi\phi$ , is expressed as:

$$\tau_{b,flush} = (0.3 + 15 \frac{A_{ss}}{s\phi})\sqrt{f_c} \leq 0.7\sqrt{f_c} \quad (1)$$

$$\tau_{b,mid-barrel} = (0.1 + 15 \frac{A_{ss}}{s\phi})\sqrt{f_c} \leq 0.7\sqrt{f_c} \quad (2)$$

where the characteristic bond resistance specified in the British Code,  $0.7\sqrt{f_c}$ , was chosen as the upper bound value. As mentioned before, the dimensionless function ( $A_{ss}/(s\phi)$ ) was used to express the stirrup restraint, where the effective stirrup area,  $A_{ss}$ , was suggested to be equal to the stirrup

area,  $A_{sw}$ , for a single or bundled bar placed at the bent of a stirrup and equal to zero when placed away from the bent of the stirrups. Its extensions to other cases were to a greater or lesser extent justified by Regan and Kennedy Reid. It is important to note that the corrosion of stirrups, which is often severe at their bends and may cause a loss of anchorage, is not accounted for. The authors further clarify that the proposed bond stresses do not yield characteristic values. They are, however, intended to be used in the analysis of beams and slabs to predict ultimate loads, which can reasonably be regarded as at a characteristic level, provided that the models in which they are used are in equilibrium and respect other relevant stress limits. A comparison of the bond strength after cover spalling based on the empirical model of Regan and Kennedy Reid and the analytical model of Lundgren et al. (2012) for varying transverse reinforcement contents and compressive strength is shown in Figure 1. The empirical model does not account for any additional confining effect for a transverse reinforcement content exceeding 0.04. However, the analytical model relies on the additional confining effect of transverse reinforcement even for  $A_{sw}/s\phi$  higher than 0.04, provided that a ‘good’ bond condition is assumed. Overall, the prediction of the two models seems to highly depend on compressive strength, as well as the choice of spalling pattern (‘flush’ and ‘mid-barrel’) and bond conditions (‘good’ or ‘all other’). The predictions of the models are later compared with experimental data and numerical simulations in Section 5.2.

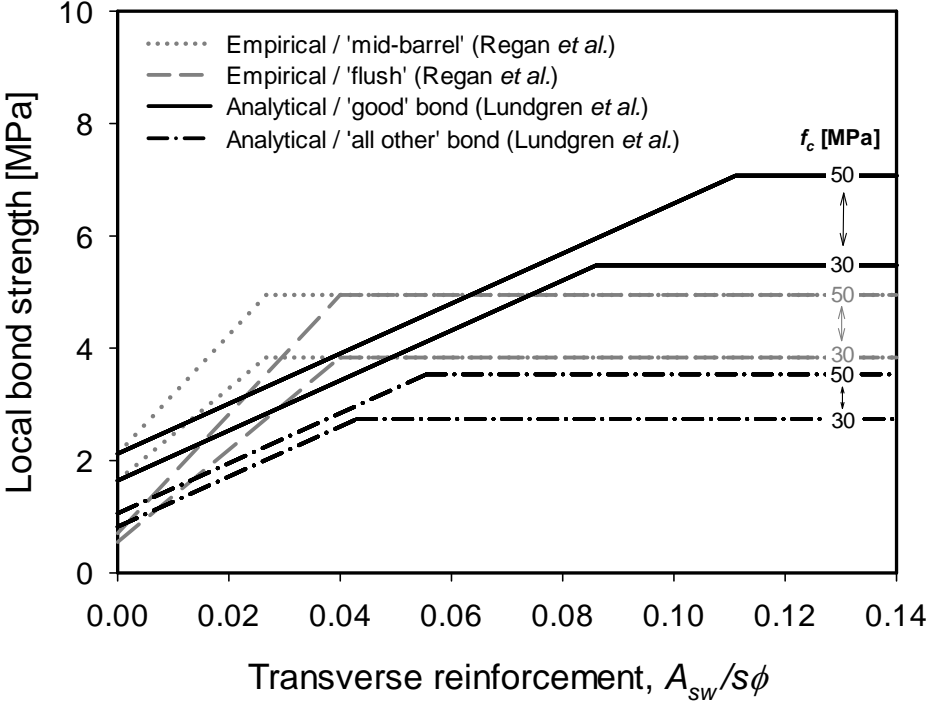


Figure 1. Comparison of the empirical and analytical models for bond strength after cover spalling by Regan and Kennedy Reid (2009) and Lundgren et al. (2012), respectively.

### 3 Numerical modelling of anchorage, corrosion and spalling

The anchorage capacity of deformed bars in concrete is strongly influenced by the actual confinement conditions. In general, confinement is the result of the surrounding concrete, stirrups and transverse pressure. Corrosion of reinforcement leads to volume expansion of the steel, which generates splitting stresses in the concrete, something that influences the bond between the concrete and reinforcement. At a larger corrosion penetration, the splitting stresses may lead to cover cracking

and, finally, spalling of the concrete cover. While the corrosion of longitudinal reinforcement influences the bond and subsequent composite action, the corrosion of stirrups weakens the confinement due to the combined reduction in the cross-sectional area of the stirrups and the extensive cover cracking resulting from the corrosion of stirrups. For a natural corrosive environment, in which both longitudinal and transverse reinforcements are corroded, anchorage and shear failures become more probable. These effects can be included in the analysis of reinforced concrete members with corrosion-induced cover spalling using different approaches with varying degrees of detail.

Three-dimensional finite element modelling has proven to be capable of describing the behaviour of reinforced concrete in a comprehensive way provided that appropriate constitutive models have been adopted. Furthermore, the effect of corrosion on the reinforcement, the surrounding concrete and their interaction can more realistically be simulated. Although detailed structural analyses are numerically expensive, they allow for a more accurate description of the corrosion damage at the material and structural levels. Volume expansion of corrosion products, leading to cover cracking and spalling, significantly influences the confinement conditions and consequently the steel/concrete bond. These effects were taken into account in bond and corrosion models previously developed by Lundgren (2005a, 2005b), and thereafter extended by Zandi Hanjari et al. (2013). In this study, these models were combined with a computation scheme to simulate the effect of corrosion-induced cover spalling on anchorage capacity. A short overview of the previous developments of the model followed by the proposed computation scheme for corrosion-induced cover spalling is provided below.

#### 4 Overview of earlier developments of the model

In earlier studies (Lundgren & Gylltoft, 2000), a general model of the bond mechanism was developed; the model was later combined with the modelling of corrosion attacks on reinforcement (Lundgren, 2005a; Lundgren, 2005b). The modelling approach was especially suited for detailed 3D FE analyses, in which both concrete and reinforcement were modelled by using solid elements, see Figure 2(a). Surface interface elements were used at the steel/concrete interaction to describe a relationship between the stresses,  $\sigma$ , and the relative displacement,  $u$ , in the interface, Equations (16-18) in Figure 2. The corrosion and bond models can be viewed as two separate layers around a reinforcement bar. Due to an equilibrium between the two layers, the stress,  $\sigma$ , is the same in the bond and corrosion layers. The deformations in the bond and corrosion layers were solved in the interface element together with the condition for equilibrium by using an iterative procedure, Equation (19) in Figure 2.

The bond model (Lundgren, 2005a) is a frictional model describing the relationship between stresses and deformations based on elasto-plastic theory, see Figure 2(b). The yield lines of the model were described by two yield functions: one describing the friction,  $F1$ , assuming that the adhesion was negligible, and the other,  $F2$ , describing the upper limit for a pull-out failure determined by the stress in the inclined compressive struts resulting from the bond action, Equations (20-21) in Figure 2. Consequently, the bond stress depended not only on the slip, but also on the radial deformation between the reinforcement bar and concrete. Thus, the loss of bond at splitting failure or reinforcement yielding could be accounted for.

The corrosion model simulates the effect of corrosion as the volume increase of the corrosion products compared to the virgin steel (Lundgren, 2005b) and accounts for the effect of corrosion products flowing through the cracks (Zandi Hanjari et al., 2013). The volume of the corrosion products relative to the uncorroded steel,  $v_{rs}$ , the corrosion penetration depth into the steel bar,  $x$ , as a function of time and the volume of corrosion products flowing through a crack,  $V$ , are used to calculate the free increase of the bar radius,  $y_{ext}$ , see Figure 2(c) and Equation (22). The corrosion time, i.e. duration of the corrosion process, and corrosion rate, i.e. the depth of corrosion penetration into the steel bar per unit of time, are inputs to the model and the corrosion penetration depth,  $x$ , is determined theoretically based on Faraday's law in Equations (23). The total strain in the corrosion products,  $\epsilon_{cor}$ , is then calculated using Equation (24), and the corresponding stresses normal to the bar surface are determined based on the normal strain in the corrosion products, Equation (25).

The volume of corrosion products that flows through a crack,  $V$ , is assumed to depend on the crack

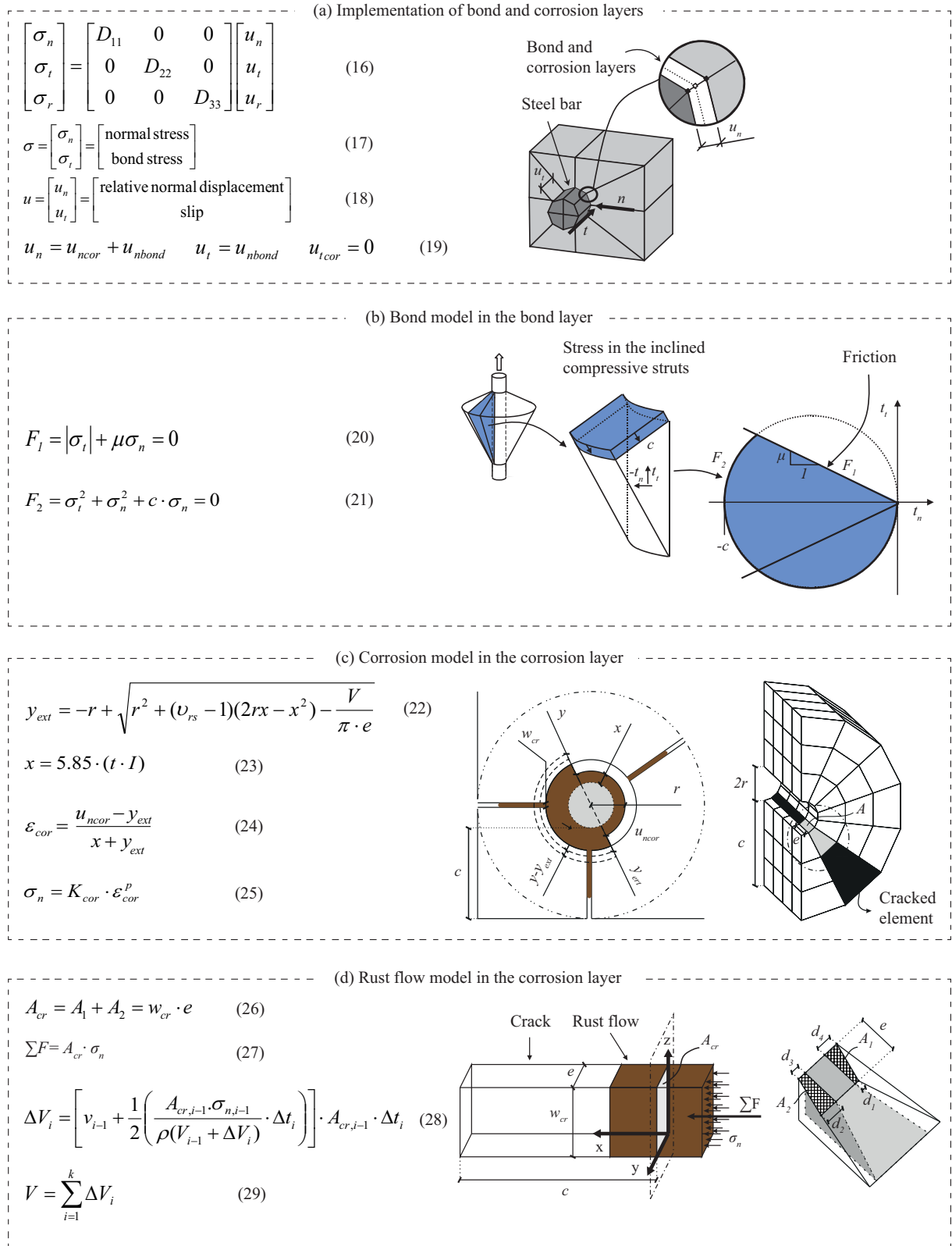


Figure 2. General overview of the model developments: (a) implementation of bond and corrosion layers (Lundgren, 2005a), (b) bond model in the bond layer (Lundgren, 2005a), (c) corrosion model in the corrosion layer (Zandi Hanjari *et al.*, 2013), and (d) rust flow model in the corrosion layer (Zandi Hanjari *et al.*, 2013).

width and normal stress in the corrosion products; see Figure 2(d). The crack width closest to the bar,  $w_{cr}$ , is computed from the nodal displacements across the crack. It is assumed that the crack had a constant width of  $w_{cr}$  along its depth. The cross-sectional area of the crack through which corrosion products flow is then calculated as in Equation (26). A one-dimensional flow based on a plug flow model, i.e. the constant velocity of the flow of the corrosion products along a crack, is applied to calculate the volume flow of corrosion products. The motion of the corrosion products is described by the Lagrangian formulation. The phenomenon is expressed as an ideal flow, i.e. the friction in the crack is assumed to be negligible. The motion of corrosion product particles is assumed to be driven by the normal stress in the corrosion products,  $\sigma_n$ ; thus, the external force acting on the section area of the crack is calculated as in Equation (27). The amount of corrosion products transported across the section area of the crack is then computed in time steps in Equation (28), and the total volume flow of corrosion products,  $V$ , through a crack in Equation (29).

## 5 Computation scheme for corrosion-induced cover spalling

Finite element analysis based on smeared crack formulations, including the rotating crack model, has difficulties in correctly representing geometrical discontinuity after the tensile softening of a finite element has been completed. This results in a too stiff response at cracking due to a spurious stress transfer, so-called stress locking, and spurious kinematic modes at spalling, so-called numerical instability, because of a violation of the displacement continuity assumption. A possibility of overcoming stress locking in the smeared crack approach would be to remove finite elements from the mesh as soon as their tensile softening had been completed (Rots, 1988). With this technique, a gap would propagate through the mesh behind the micro crack and the concrete at either side of the crack would be elastically unloaded (Rots, 1992). In this paper, a similar approach is adopted that allows for possible changes in the topology of the mesh as corrosion-induced cracks connect and form a delamination plane.

A computation scheme for a three-dimensional non-linear FE analysis is devised which comprises several calculation phases. Each load step is applied within one calculation phase. In each phase, a separate analysis is performed and the results from previous phases, typically stresses, are imposed as initial values. Between each phase, a new finite element mesh is adapted excluding the elements that have completed their tensile softening and those that belong to a delaminated part. However, these elements are excluded from the mesh only after a delamination plane has been formed; in this respect, the approach differs from that devised by Rots (1992), by leading to a more stable analysis with enormous savings in computing time. Therefore, the poor kinematic representation of the discontinuous displacement field around a delamination plane after full tensile softening has been successfully avoided. The computation scheme is outlined in Figure 3.

The examples provided in Figure 3 correspond to eccentric pull-out specimens who have the shape of beam-ends after inclined shear cracking (Coronelli et al., 2013; Zandi Hanjari et al., 2011a). The two specimens differ with respect to the amount of longitudinal reinforcement; one with no stirrups along the embedment length (Type I) and the other with four stirrups along the embedment length (Type II). A detailed finite element analysis of these specimens, based on the approach summarized in Section 4.3.1, has been presented by Zandi Hanjari et al. (2013). The analyses could only be carried out to a corrosion attack equivalent to rebar weight losses of around 10% and 15% for the specimens of Type I and II, respectively. These corrosion levels corresponded to extensive cover cracking, see Figures 3(g) and 5(h). For higher corrosion attacks, the cracks would connect and form a delamination plane and result in numerical instability in the analyses. However, the analyses with the proposed computation scheme could be continued with larger corrosion penetration depths to compute corrosion-induced cover spalling as shown in Figures 3(i) and 5(j). The overall cracking and spalling patterns depended on bar diameter, bar spacing and concrete cover as described by Du et al. (2013). The difference in the spalling pattern in the two types of specimens was related to the amount of confinement. The analysis can thus be used to study the anchorage capacity of corroded specimens with cover spalling; this is an important advantage when the proposed computation scheme is used. In general, this scheme can be used to simulate geometrical discontinuity at cracking or spalling in any given stress state, e.g. a splitting failure in a pull-out test. However, in this paper, the application of the

computation scheme is only validated for corrosion-induced cover spalling. A drawback of using this approach is the prolonged computation time; therefore, it is recommended to use it in cases when the behaviour of concrete members is of concern at or beyond cover spalling.

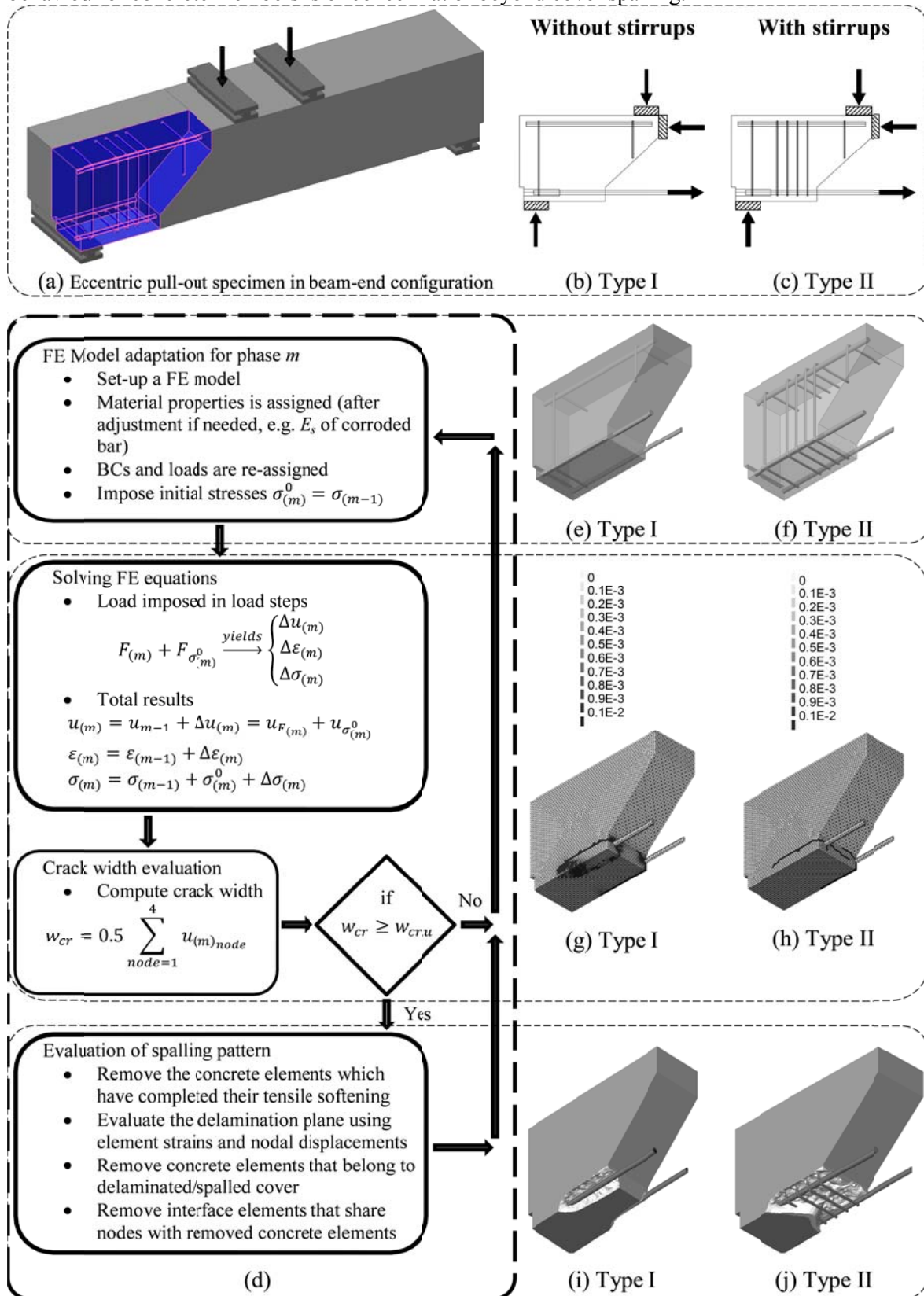
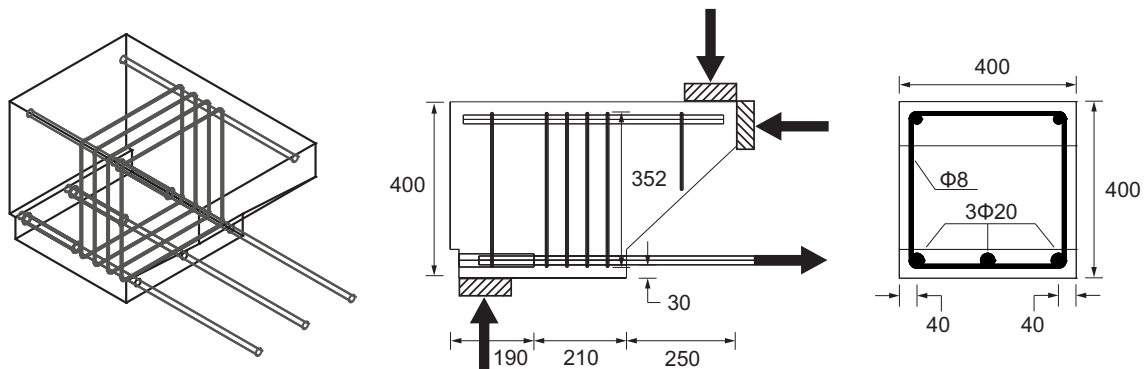


Figure 3. Computation scheme to simulate corrosion-induced cover spalling, exemplified by eccentric pull-out specimens by Coronelli *et al.* (2013) and Zandi Hanjari *et al.* (2011a).

## 6 3D FE analysis in common applications

After validation with experiments, the 3D FE analysis was used to further investigate the influence of stirrup corrosion, the variation of corrosion distribution around a bar, and the induced stresses in stirrups caused by the corrosion of main bars. The eccentric pull-out specimens tested by Coronelli *et al.* (2013) and Zandi Hanjari *et al.* (2011a) were used for this purpose; the test specimens and set-up are shown in Figure 4. The reason for such a choice was because the behaviour of these specimens share some similarities with a beam-end region, e.g. the inclined strut is carried both on the anchored bar and the support region. Moreover, the eccentric pull-out specimens enabled studying the influence of uncorroded and corroded stirrups, as well as studying the behaviour of anchored bar at middle and corner positions.



Eccentric pull-out tests by Coronelli *et al.* (2013) and Zandi Hanjari *et al.* (2011a)

Figure 4. Test specimens and set-ups with all dimensions in mm.

### ***Influence of corrosion distribution around a bar***

A non-uniform distribution of corrosion around reinforcing bars is commonly seen in RC structures exposed to aggressive environments. This might be caused, for instance, by varying concrete covers for bars located in corner positions, variations in the surrounding environment, or direct access from the aggressive environment to a bar due to pre-existing cracks. On the other hand, measuring corrosion distributions using conventional measurement techniques, such as gravimetric methods, is challenging and not always practically possible. Thus, the influence of varying corrosion distributions around a bar on the bond strength was investigated using a 3D FE analysis of the eccentric pull-out specimens. Four corrosion distributions, namely full, three-quarter, half and one-quarter of the surface area of the bar, were analysed and the same corrosion weight loss was imposed in all cases.

The result of these 3D FE analyses in terms of normalized bond strength, as shown in Figure 5, indicates that the bond strength is only slightly influenced by corrosion distribution. The same observation holds true when the crack patterns, not shown here, were compared. This finding can be explained by the equilibrium between the bar and surrounding concrete which remains nearly the same independent of the pressure distribution around the bar. Accordingly, the same stress state is expected in the analysis of different corrosion distributions resulting in the same bond strength, whereas if the same corrosion penetration, instead of corrosion weight loss, were imposed on the bar with varying distributions, the resultant pressure would depend on the corrosion distribution, as would the stress state and bond strength. It should be noted that highly localized corrosion, concentrated over a much smaller surface area than a quarter of a bar circumference, may induce large and localized strains in the bar (known as a notch effect) for which the conclusion made for the four cases studied will no longer hold true.

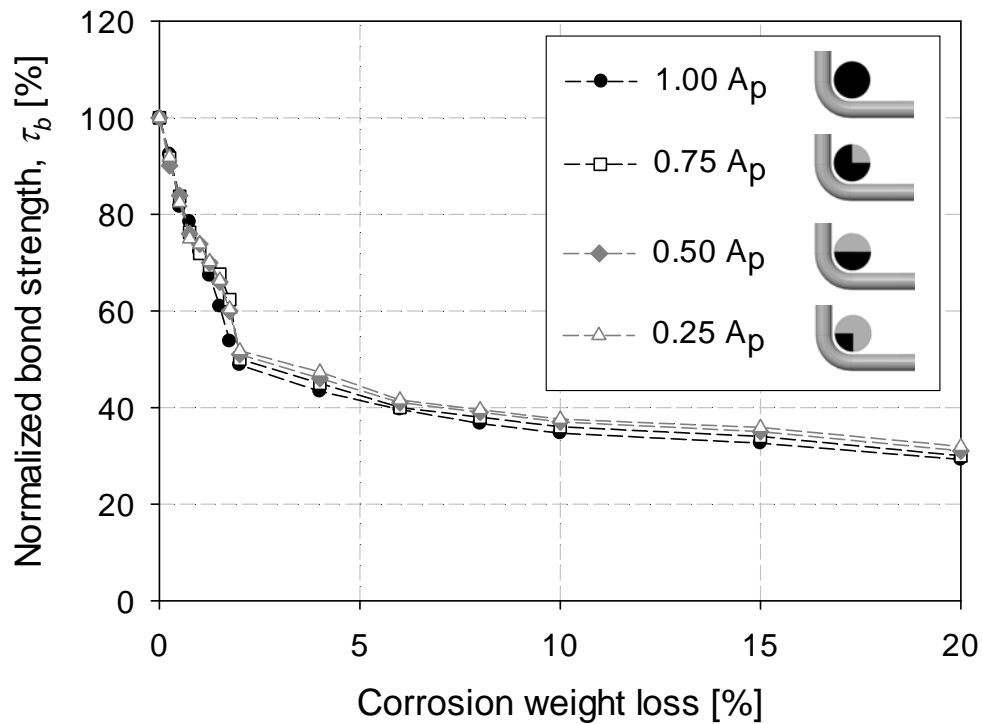


Figure 5. Influence of corrosion distribution around a bar on the bond strength, based on the 3D FE analysis of eccentric pull-out specimens by Coronelli *et al.* (2013) and Zandi Hanjari *et al.* (2011a). The black parts of the bars were subjected to corrosion.

#### ***Effect of corrosion of stirrups on bond capacity***

A rather common approach in modelling the effect of corroded stirrups is to take into account the loss of the cross-sectional area. However, this does not account for the volume expansion of rust around the corroded stirrups, which may lead to cover cracking and spalling. Field investigations and laboratory tests have shown that cover delamination is more probable in areas with corroded stirrups, particularly when the stirrups are closely spaced (Higgins and Farrow III, 2006). Thus, the influence of corroded stirrups on bond strength was studied using a 3D FE analysis of the eccentric pull-out specimens. The analyses were carried out for specimens with no stirrups (Type I), with four uncorroded stirrups (Type II), and with four corroded stirrups (Type III) along the embedment length. The stirrups were modelled according to the same level of detail as the main bars, which allowed for a simulation of the effect of corroded stirrups. The same corrosion penetration was imposed on main bars and stirrups.

The results in terms of normalized bond strength, as shown in Figure 6, indicate that the corrosion of stirrups advances cracking and spalling and results in higher bond deterioration at the early stages of corrosion. However, when the cover is fully cracked or spalled off, the corrosion of the stirrups does not remarkably influence the bond capacity for higher levels of corrosion. This is because stirrups become the primary source of confinement after cover cracking or spalling. These observations seem to hold true regardless of whether a corner or middle bar is of concern, see Figures 6(a) and 6(b), respectively. It should be noted that a more pronounced difference in bond strength may be expected if the corrosion of stirrups would cause early yielding; however, this was not the case in the analyses presented. After all, the corrosion of stirrups is more likely to have a prominent influence in particular on the shear capacity of RC structures through a reduction in the sectional area of stirrups than on the anchorage capacity of main bar. Additionally, the induced stresses in stirrups as a result of the

corrosion in neighbouring bars, which is studied in the following section, may also influence the shear capacity of RC members.

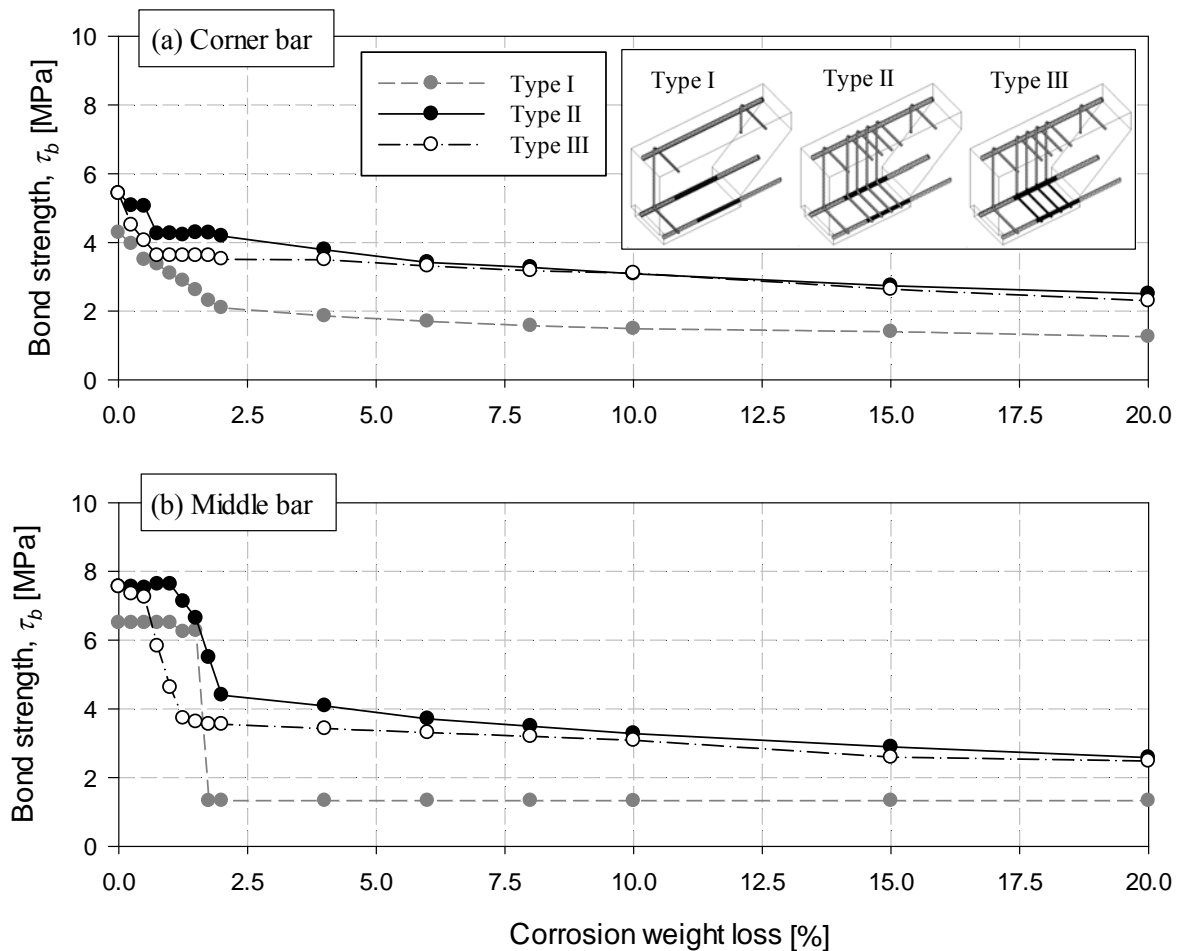


Figure 6. Influence of corrosion of stirrups on bond strength, based on 3D FE analysis of eccentric pull-out specimens by Coronelli *et al.* (2013) and Zandi Hanjari *et al.* (2011a). The black parts of bars and stirrups were subjected to corrosion.

#### ***Stress in stirrup due to corrosion in longitudinal bar***

The expansion that takes place around a corroded bar may result in not only splitting stresses in the surrounding concrete but may also cause tensile forces in neighbouring bars. If the magnitude of the stresses induced in the stirrups due to corrosion of adjacent bars were to become significant, there is a risk for a major reduction in the shear capacity of a corroded RC member. The effect of corrosion of main bars on stresses in a transverse reinforcement was studied using a 3D FE analysis of the eccentric pull-out specimens. The variation of stresses in stirrups due to 2, 5, 10 and 20% corrosion weight loss in the main bars is shown in Figure 7. The results are shown for two cross-sections, one with two corroding bars on the bottom, see Figure 7(a), and another with three corroding bars on the bottom and one corroding bar on the top of the concrete cross-section, see Figure 7(b).

The results show that stresses in a stirrup may reach as high as 80 MPa (approximately 15% of yield stress) when the main bars are subjected to 20% corrosion weight loss. However, these stresses rapidly diminish within a short distance from the corroded bar. Thus, the shear capacity of a corroded RC member may be influenced by the corrosion of main bars only if shear cracks come across stirrups at a location with high stresses. Moreover, it can be seen in Figure 7(b) that closely spaced corroded main bars may lead to high stresses over a greater stirrup length. On the other hand, 20% corrosion weight loss of a 20 mm main bar is equivalent to approximately 25% corrosion weight loss of an 8 mm

stirrup, both corresponding to around 1000  $\mu\text{m}$  corrosion penetration. Hence, if the stirrups were also to corrode, the reduction in cross-sectional area would have led to approximately 25% decrease in the stirrups yield force; this is in addition to the influence of corroded stirrups on early cover cracking and spalling which described in Section 6.2. Consequently, the corrosion of stirrups seems to influence the behaviour of an RC member more prominent than the induced stresses in stirrups due to the corrosion of main bars.

It was also observed that the stresses induced in stirrups because of the corrosion of several corroding bars located at varying distances can be estimated by superimposing the influence of each as long as the stresses induced remain below the yield stress within the elastic region. The stresses induced in stirrups are expected to grow with an increased diameter of main bar or a decreased diameter of stirrups. Nonetheless, it is unlikely for stirrups to yield because of the corrosion of main bars if conventional bar diameters for stirrups and main bars, as well as common reinforcement arrangement (spacing) were employed.

The shear capacity of beams with corroded stirrups was studied in an experimental program by Higgins and Farrow III (2006) in which stirrups were subjected to corrosion while the corrosion of the flexural reinforcements was prevented. Extensive cracking, partial delamination and staining were observed for sectional losses of stirrups of 12%, 20% and 40%; this finding agrees with the observation described in Section 6.2. These authors showed that when stirrups were subjected to corrosion, the spacing of the stirrups governed the extent of damage to the concrete cover. In regions with tightly spaced stirrups, the cover cracks from neighbouring stirrups interacted and caused larger areas of spalling and delamination. When stirrups were widely spaced, the damage to the concrete cover was more localized. Higgins and Farrow III also showed that when the stirrups were highly corroded, the capacity of the beams was reduced by up to 50%. It may be concluded that corrosion may influence the shear capacity of an RC member not only due to a reduction of the cross-sectional area of corroded stirrups, but also due to stresses in stirrups as the result of corrosion in the main bars. However, the influence of the corrosion of stirrups on shear capacity is expected to be much more pronounced than that of stirrup stresses induced due to corrosion of the main bar.

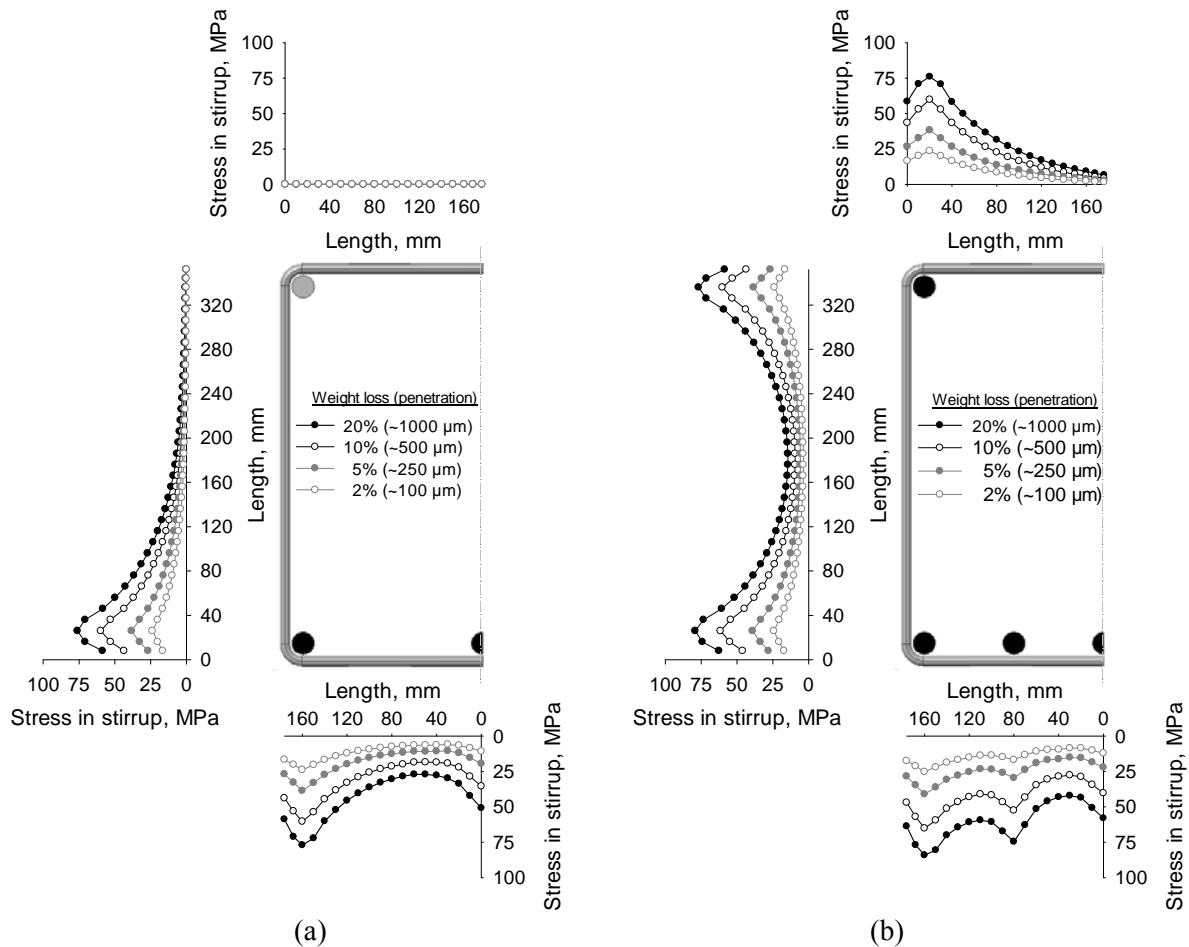


Figure 7. The influence of corrosion of main bar on the stresses in stirrups, based on 3D FE analysis of eccentric pull-out specimens by Coronelli *et al.* (2013) and Zandi Hanjari *et al.* (2011a). The black bars were subjected to corrosion.

## 7 Conclusion

When RC structures are exposed to highly corrosive environments, the splitting stresses around corroded bars may lead to cover cracking and ultimately cover spalling, thereby altering the resistant mechanism in the cross-section; stirrups then become the primary source of confinement. The anchorage capacity of corroded RC structures is thus influenced by cover cracking, cover spalling, as well as by the corrosion of stirrups. The structural consequences of corrosion-induced cover spalling and corroded stirrups have been investigated in this paper. The following conclusions are drawn on the basis of this study:

- corrosion of stirrups advances the time to cracking and spalling, while bond strength is only slightly influenced by stirrup's corrosion after cover spalling,
- bond strength is not significantly influenced by a varied corrosion distribution around a bar, as long as the same corrosion weight loss is imposed at a given cross-section independently of the corrosion distribution, and that
- stresses in stirrups due to the corrosion of adjacent bars rapidly diminish within a short distance of the main bar and the magnitude of these stresses depends on the spacing of the main bar.

## References

- Al-Sulaimani, G.J., Kaleemullah, M., Basunbul, I.A., & Rasheeduzzafar. (1990). Influence of corrosion and cracking on bond behavior and strength of reinforced concrete members. *ACI Structural Journal*, 87 (2), 220-231.
- Almusallam, A.A. (2001). Effect of degree of corrosion on the properties of reinforcing steel bars. *Construction and Building Materials*, 15 (8), 361-368.
- Almusallam, A.A., Algahtani, A.S., Aziz, A.R., Dakhil, F.H., & Rasheeduzzafar. (1996). Effect of reinforcement corrosion on flexural behavior of concrete slabs. *Journal of Materials in Civil Engineering*, 8 (3), 123-127.
- Andrade, C., Alonso, C., & Molina, F.J. (1993). Cover cracking as a function of bar corrosion - 1. Experimental test. *Materials and Structures*, 26 (162), 453-464.
- Cabrera, J.G., & Ghoddoussi, P. (1992). The effect of reinforcement corrosion on the strength of the steel/concrete 'bond'. *Bond in Concrete, Proceedings of an International Conference, Riga, Latvia, 10-11 – 10-24*.
- Cairns, J., Plizzari, G.A., Du, Y., Law, D.W., & Franzoni, C. (2005). Mechanical properties of corrosion-damaged reinforcement. *ACI Materials Journal*, 102 (4), 256-264.
- Cairns, J., & Zhao, Z. (1993). Behaviour of concrete beams with exposed reinforcement. *Proceedings of the Institution of Civil Engineers, Structures and Buildings*, 99 (2), 141-154.
- CEB. (1993). CEB-FIP Model Code 1990. *Bulletin d'Information 213/214*, Lausanne, Switzerland.
- CEB. (2013). CEB-FIP Model Code 2010. *Fib Bulletin 55: Wilhelm Ernst & Sohn, Verlag für Architektur*, Lausanne, Switzerland.
- Clark, L.A., & Saifullah, M. (1993). Effect of corrosion on reinforcement bond strength. In Forde, M. (Ed.), *5th International Conference on Structural Faults and Repairs*. Edinburgh: Engineering Technical Press, 113-119.
- Coronelli, D., & Gambarova, P. (2004). Structural assessment of corroded reinforced concrete beams: Modeling guidelines. *Journal of Structural Engineering*, 130 (8), 1214.
- Coronelli, D., Zandi Hanjari, K., Lundgren, K., & Rossi, E. (2011). Severely corroded reinforced concrete with cover cracking: Part 1. Crack initiation and propagation. In Andrade, C. & Mancini, G. (Eds.), *Modelling of Corroding Concrete Structures*. 195-205.
- Coronelli, D., Zandi Hanjari, K., & Lundgren, K. (2013). Severely corroded RC with cover cracking. *Journal of Structural Engineering–ASCE*, 139 (2), 221-232.
- Du, Y.G. (2001). Effect of reinforcement corrosion on structural concrete ductility. Doctoral thesis, University of Birmingham, UK.
- Du, Y.G., Chan, A.H.C., Clark, L.A., Wang, X.T., Gurkalo, F., & Bartos, S. (2013). Finite element analysis of cracking and delamination of concrete beam due to steel corrosion. *Engineering Structures*, 56, 8-21.
- Du, Y.G., Clark, L.A., & Chan, A.H.C. (2005). Effect of corrosion on ductility of reinforcing bars. *Magazine of Concrete Research*, 57 (7), 407-419.
- International Federation for Structural Concrete (fib) Bulletin 10. (2000). *Bond of Reinforcement in Concrete, state-of-art report*. Fédération internationale du béton, prepared by Task Group Bond Models, Lausanne, 427 p.
- Higgins, C., & Farrow III, W.C. (2006). Tests of reinforced concrete beams with corrosion-damaged stirrups. *ACI Structural Journal*, 103 (1), 133-141.
- Lundgren, K. (2005a). Bond between ribbed bars and concrete. Part 1: Modified model. *Magazine of Concrete Research*, 57 (7), 371-382.
- Lundgren, K. (2005b). Bond between ribbed bars and concrete. Part 2: The effect of corrosion. *Magazine of Concrete Research*, 57 (7), 383-395.
- Lundgren, K. (2007). Effect of corrosion on the bond between steel and concrete: An overview. *Magazine of Concrete Research*, 59 (6), 447-461.
- Lundgren, K., & Gylltoft, K. (2000). A model for the bond between concrete and reinforcement. *Magazine of Concrete Research*, 52 (1), 53-63.
- Lundgren, K., Kettil, P., Zandi Hanjari, K., Schlune, H., & San Roman, A.S. (2012). Analytical model for the bond-slip behaviour of corroded ribbed reinforcement. *Structure and Infrastructure Engineering*, 8 (2), 157-169.

- Molina, F.J., Alonso, C., & Andrade, C. (1993). Cover cracking as a function of rebar corrosion. 2. Numerical model. *Materials and Structures*, 26 (163), 532-548.
- Rasheeduzzafar, Al-Saadoun, S.S., & Al-Gahtani, A.S. (1992). Corrosion cracking in relation to bar diameter, cover, and concrete quality. *Journal of Materials in Civil Engineering*, 4 (4), 327-342.
- Regan, P.E., & Kennedy Reid, I. (2004). Shear strength of RC beams with defective stirrup anchorages. *Magazine of Concrete Research*, 56 (3), 159-166.
- Regan, P.E., & Kennedy Reid, I. (2009). Assessment of concrete structures affected by delamination: 1 - effect of bond loss. *Studies and Research - Annual Review of Structural Concrete*, 29, 245-275.
- Regan, P.E., & Kennedy Reid, I. (2010). Assessment of concrete structures affected by delamination: 2 - bond-shear interaction. *Studies and Research - Annual Review of Structural Concrete*, 30.
- Rodriguez, J., Ortega, L.M., & Casal, J. (1995). The residual service life of reinforced concrete structures: Relation between corrosion and load bearing capacity of concrete beams. *The Residual Service Live of Reinforced Concrete Structures*. 33.
- Rodriguez, J., Ortega, L.M., & Casal, J. (1997). Load carrying capacity of concrete structures with corroded reinforcement. *Construction and Building Materials*, 11 (4), 239-248.
- Rots, J.G. (1988). Computational modeling of concrete fracture. Doctoral thesis, Delft University of Technology, Delft, Netherland.
- Rots, J.G. (1992). Removal of finite elements in strain-softening analysis of tensile fracture. In Bazant, I.Z.P. (Ed.), *Fracture Mechanics of Concrete Structures*. London and New York, 330-338.
- Sæther, I. (2009). Bond deterioration of corroded steel bars in concrete. *Structure and Infrastructure Engineering*, 7 (6), 415-429.
- Silva, N. (2013). Chloride induced corrosion of reinforcement steel in concrete - threshold values and ion distributions at the concrete-steel interface. Doctoral thesis, Chalmers University of Technology, Göteborg, Sweden.
- Sustainable Bridges. (2007). D4.2 Guideline for load and resistance assessment of existing European railway bridges - advices on the use of advanced methods: Prepared by WP4, No. TIP3-CT-2003-001653.
- Tuutti, K. (1982). Corrosion of steel in concrete: CBI Swedish Cement and Concrete Research Institute, Borås, Sweden.
- Zandi Hanjari, K. (2010). Structural behaviour of deteriorated concrete structures. Doctoral thesis, Chalmers University of Technology, Göteborg, Sweden.
- Zandi Hanjari, K., Coronelli, D., & Lundgren, K. (2011a). Bond capacity of severely corroded bars with corroded stirrups. *Magazine of Concrete Research*, 63 (12), 953-968.
- Zandi Hanjari, K., Kettil, P., & Lundgren, K. (2011b). Analysis of mechanical behavior of corroded reinforced concrete structures. *ACI Structural Journal*, 108 (5), 532-541.
- Zandi Hanjari, K., Lundgren, K., Plos, M. & Coronelli, D. (2013). Three-dimensional modelling of structural effects of corroding steel reinforcement in concrete. *Structure and Infrastructure Engineering*, 9 (7), 702-718.